Subsecond Time-resolved Photometry of Tiny Near-Earth Objects with Tomo-e Gozen.

Jin Beniyama[1], Shigeyuki Sako[1], Ryou Ohsawa[1], Satoshi Takita[1], Naoto Kobayashi[1], Shin-ichiro Okumura[2], Seitaro Urakawa[2], Makoto Yoshikawa[3], Fumihiko Usui[3], and Fumi Yoshida[4,5] ,
[1]Institute of Astronomy, Graduate School of Science, The University of Tokyo, 2-21-1 Osawa, Mitaka, Tokyo, 181-0015, Japan, beniyama@ioa.s.u-tokyo.ac.jp, [2]Japan Spaceguard Association, [3]Institute of Space and Astronautical Science, Japan Aerospace Exploration Agency,[4]University of Occupational and Environmental Health, [5]Planetary Exploration Research Center, Chiba Institute of Technology

Introduction: As of December 2021, 27800 near-Earth objects (NEOs) have been discovered [1] by wide-field monitoring surveys such as Catalina Sky Survey [2] and Pan-STARRS [3]. Most NEOs have their origins in the main belt [4]. Asteroidal fragments are generated from collisional events in the main belt and their orbital elements are gradually changed by the Yarkovsky effect [5]. When the asteroids enter into orbital resonances with giant planets, their orbits evolve to those of NEOs in a few Myr [6].

During the orbital evolution, the rotation states of the asteroid are changed by the Yarkovsky-O'Keefe-Radzievskii-Paddack (YORP) effect [7]. Since the strength of the YORP effect increases with decreasing diameter, smaller asteroids have been experienced larger change in the rotation states. The rotation acceleration by YORP leads to deformation or rotational fission of the asteroid due to a strong centrifugal force. Because the strength of YORP effect is also dependent on physical properties such as shape and thermal conductivity, the rotation period distribution of smaller objects probably reflects the dynamical history and physical properties.

In general, it is difficult to constrain the rotation states of tiny (diameter smaller than 100 m) asteroids due to the limited observational windows, the fast rotations, and the large apparent motions on the sky. For asteroids larger than 200 m in diameter, the rotation period distribution is truncated around 2 hours. This clear structure is called the cohesionless spin barrier and indicates most of the larger asteroids are rubble-piles [8]. Although it is possible to constrain physical properties of asteroids smaller than 200 m in diameter as well, the number of asteroids for which the rotation period has been reported is limited. Recently, Mission Accessible Near-Earth Objects Survey (MANOS) obtained more than 300 light curves of small NEOs (mean absolute magnitude $H \sim 24$) using large and medium aperture telescopes [9, 10]. Although MANOS successfully derived the rotation periods of NEOs with high accuracy, the survey was not optimized to detect faint and fast rotators. Due to a relatively long exposure time (1–300 s), the survey possibly undetected the very fast rotations. Systematic high-speed observations are required to correctly derive shorter rotation periods of tiny NEOs.

Observations: We conducted photometric observations at 2 fps with the wide-field CMOS camera Tomo-e Gozen mounted on the 105 cm Schmidt telescope at Kiso Observatory in Nagano, Japan [11]. We have obtained light curves of 60 NEOs (hereinafter referred to as the Tomo-e NEOs) from May 2018 to October 2021. Nominal criteria for target selection are that V-band apparent magnitude $V < 17$ and an absolute magnitude $H > 22.5$. We set a nominal duration of observation as 20 min. The Tomo-e NEOs were typically located at a few lunar distances from Earth and a typical angular velocity was about a few arcsec/s when observed.

Data reduction: After bias and dark subtraction and flat-field correction, the standard circle aperture photometry was performed on a target and reference stars in each frame of video data using the SExtractor-based python package `sep` [12, 13]. We used the G-band magnitude of Gaia DR2 catalog as brightness references [14]. We applied the Lomb-Scargle technique to estimate rotation periods from non-evenly sampled data [15, 16]. For optimal determination of the number of harmonics, we used Akaike Information Criterion (*AIC*, [17]). The uncertainty of the rotation period and the light curve amplitude were estimated using the Monte Carlo method.

Results: We successfully derived the rotation periods of 32 samples. The rotation periods of 18 objects were not derived due to small amplitude and we found 10 candidates of tumbler.

Light curves : We found 13 samples with rotation periods less than 60 s. Thanks to the video observations at 2 fps, we can estimate such a short rotation period with high reliability. As an example, the rotation period of 2021 CG was estimated to be 15.296 ± 0.002 s. The light curve folded by the rotation period is shown in Figure 1.

Diameter and rotation period (D-P) relation : The D-P relation of the Tomo-e NEOs and the NEOs in the Asteroid Light Curve Database (LCDB, [18]) is shown in figure 2. We performed the Kolmogorov-Smirnov (KS) test to check the null hypothesis that the two D-P relations are the same. We chose the NEOs satisfying the criteria that $H > 22.5$ and $P < 420$ s corresponding to the longest rotation period of the Tomo-e NEOs. This tentatively implies that rotation periods of some fast rotators have not been able to be estimated due to long exposure time observations in the previous studies.

Axial ratios : No strong correlation is seen in both *H* vs. a/b and *P* vs. a/b. This results are consistent with previous studies [9, 19].

Discussions: Although we can derive short rotation periods approximately up to 1.5 s in our systematic 20 min video observations, we found only one NEO with rotation periods shorter than 10 s. The distribution of the Tomo-e NEOs in the D-P relation is truncated around 10 s in the rotation period as shown in Figure 2. To interpret this flat-top distribution, we performed model calculations taking into account the YORP effect. Based on the calculations, tiny NEOs with diameters less than 10 m and ages older than 10 Myr, corresponding to the typical dynamical evolution timescale of the NEOs, rotates faster than 10 s.

We discuss the possibility that fast-rotating tiny asteroids are destroyed by the centrifugal force [20] and the YORP acceleration can be suppressed by meteoroid impacts onto an asteroid surface [21]. As a result, the flat-top shape of the distribution is not reproduced in either case.

Recently, the tangential YORP (TYORP) effect, which is caused by a recoil force parallel to the surface, was proposed [22]. In most cases, TYORP contributes to the acceleration of the rotation under certain conditions unlike NYORP, which decelerates the rotation as well [22, 23]. The observed truncation around 10 s in rotation period may be produced by the TYORP effect (solid line in Figure 2).

Conclusions: A rotation period of an asteroid reflects its dynamical history and physical properties. We have obtained the light curves of 60 tiny (diameter smaller than 100 m) NEOs and successfully derived the rotation periods and axial ratios of 32 samples owing to the video observations at 2 fps. We discovered that the distribution of the tiny NEOs in the D-P diagram is truncated around a period of 10 s. The truncated distribution is not well explained by either the realistic tensile strength of NEOs or the suppression of YORP by meteoroid impacts. We found that the tangential YORP effect is a possible mechanism to produce the truncated distribution, although further observational and theoretical studies are necessary to reach the conclusion.

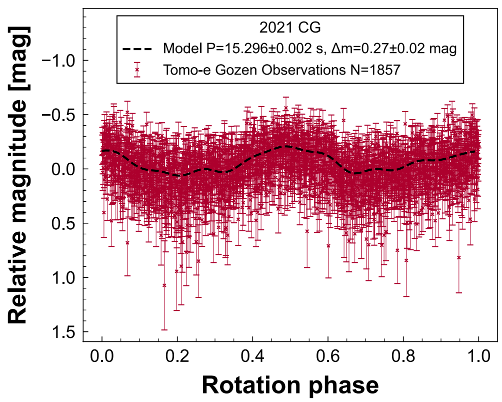

Figure 1. Phased light curve of 2021 CG. Bars indicate the 1 sigma uncertainties. A model curve with a period of 15.296 s and a light curve amplitude of 0.27 mag is shown by a dashed line.

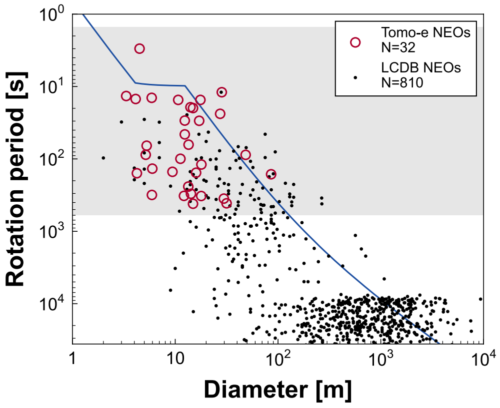

Figure 2. Diameter and rotation period (D-P) relations of the Tomo-e NEOs (open circles) and the NEOs in LCDB (filled circles). The range of detectable rotation period, 1.5 s to 10 min, in typical observations at 2 fps for 20 min with Tomo-e Gozen is shown as a gray shaded area. Reachable rotation period considering the TYORP effect with certain parameters is presented with solid line.

References: [1] Center for Near Earth Object Studies (https://cneos.jpl.nasa.gov/stats/site_all.html) [2] Drake A. J. et al. (2009) ApJ, 696, 870 [3] Chambers K. C. et al. (2016) arXiv:1612.05560 [4] Bottke W. F. et al. (2000) Science, 288, 2190 [5] Vokrouhlický D. (1998) A&A, 335, 1093 [6] Gladman B. J. (1997) Science, 277, 197 [7] Rubincam D. P. (2000) Icarus, 148, 2 [8] Pravec P. & Harris A. (2000) Icarus, 148, 12 [9] Thirouin A. et al. (2016) AJ, 152, 163 [10] Thirouin A. et al. (2018) AJ Supplement Series, 239, 4 [11] Sako, S. et al. (2018) Society of Photo-Optical Instrumentation Engineers (SPIE) Conference Series, 10702, 107020J [12] Bertin E. & Arnouts S. (1996) A&AS, 117, 393 [13] Barbary K. et al. (2015) sep: v1.3.0 [14] Gaia Collaboration et al. (2018) A&A, 616, A1 [15] Lomb N. R. (1976), Ap&SS, 39, 447 [16] Scargle J. D. (1982) ApJ, 263, 835 [17] Akaike H. (1974) IEEE Transactions on Automatic Control, 19, 716 [18] Warner B. D. et al. (2009) Icarus, 202, 134 [19] Hatch P. & Wiegert P. A. (2015) PSS, 111, 100 [20] Holsapple K. A. (2007) Icarus, 187, 500 [21] Wiegert P. A. (2015) Icarus, 252, 22 [22] Golubov O. & Krugly Y. N. (2012) ApJL, 752, L11 [23] Golubov O. et al. (2014) ApJ, 794, 22